Chapter 12: GWA Calculations in Practice

Introduction

Importance of GW Calculations:

- Essential tool in computational condensed-matter physics.
- Predict electronic properties: band structures, spectral functions.
- Address electron correlations beyond Hartree–Fock using screening.

Introduction

Historical Context and Development:

- Originated from Hedin's seminal paper (1965).
- Correlation energies derived from polarization response of electron gas.
- Significant computational advancements since initial development.
- Exponential growth of computational power boosted practical usage.

Introduction

Challenges and Ambiguities:

- GW methods remain theoretically intricate.
- Computationally demanding, especially for complex materials.
- Improved Kohn–Sham DFT bandgaps significantly.
- Core ambiguity: determining optimal Green's function G and screened interaction W.
- Intrinsic to many-body perturbation theory; careful considerations required.

The Task: A Summary

Main Objective:

- Compute exchange-correlation self-energy:

$$\Sigma_{xc}(1,2) = iG(1,2)W(1^+,2) \tag{1}$$

- Matrix elements in independent-particle basis:

$$\Sigma_{xc,k\ell}(t_1,t_2) = i\sum_{ij} G_{ij}(t_1,t_2)W_{ij}^{k\ell}(t_1^+,t_2) \tag{2}$$

The Task: A Summary

Screened Interaction W:

$$W(r_1, r_2) = v_c(r_1, r_2) + \int dr_3 dr_4 v_c(r_1, r_3) P(r_3, r_4) W(r_4, r_2) \tag{3}$$

- Random Phase Approximation (RPA) for polarizability:

$$P \approx P_0(r_3, r_4) = -i \sum_{\sigma} G_{\sigma}(r_3, r_4) G_{\sigma}(r_4, r_3) \tag{4}$$

The Task: A Summary

Spin Considerations:

- If bare Coulomb interaction is spin-independent:

$$\Sigma_{xc,\sigma} = iG_\sigma W \tag{5}$$

- Typically start from initial guess G_0 (Kohn–Sham).
- Dyson equation for each spin component:

$$G_\sigma = G_\sigma^0 + G_\sigma^0(\Sigma_{xc,\sigma} - v_{xc,\sigma})G_\sigma \tag{6}$$

- $v_{xc,\sigma}$: Exchange-correlation potential already included.

The Task: A Summary

Fourier Transform of Self-Energy:

$$\Sigma_{xc,\sigma}(r, r'; \omega) = \lim_{\eta \to 0^+} \frac{i}{2\pi} \int d\omega' G_\sigma(r, r'; \omega + \omega') W(r, r'; \omega') e^{i\eta\omega'} \tag{7}$$

Essential Steps of GW Calculation:

1. Determine initial Green's function G_0.
2. Calculate polarizability P from G_0.
3. Solve Dyson equation for W.
4. Compute self-energy Σ_{xc} from G and W.
5. Solve Dyson/quasi-particle equation:

$$(\hat{h} + \mathrm{Re}\ \hat{\Sigma}(\varepsilon_\ell))|\psi_\ell(\varepsilon_\ell)\rangle = \varepsilon_\ell|\psi_\ell(\varepsilon_\ell)\rangle \tag{8}$$

Building on Single-Particle Green's Function G_0

Concept and Importance:

- GW self-energy ($\Sigma_{xc} = iGW$) constructed from single-particle Green's function G_0.
- G_0 typically derived from mean-field approximation or static self-energy calculation.

Building on Single-Particle Green's Function G_0

Representation of G_0:

$$G_0^\sigma(r_1, r_2; z) = \lim_{\eta \to 0^+} \sum_\ell \frac{\psi_\ell^\sigma(r_1)\psi_\ell^{\sigma *}(r_2)}{z - \varepsilon_\ell^\sigma + i\eta\, \mathrm{sgn}(\varepsilon_\ell^\sigma - \mu)} \tag{9}$$

- ψ_ℓ^σ: Single-particle eigenfunctions.
- ε_ℓ^σ: Eigenvalues.
- μ: Chemical potential.

Building on Single-Particle Green's Function G_0

Irreducible Polarizability P_0:

$$P_0(r, r'; z) = \sum_{ij\sigma} \frac{(f_{i\sigma} - f_{j\sigma})\psi^{0*}_{i\sigma}(r)\psi^{0}_{j\sigma}(r)\psi^{0}_{i\sigma}(r')\psi^{0*}_{j\sigma}(r')}{z - (\varepsilon^0_{j\sigma} - \varepsilon^0_{i\sigma})} \tag{10}$$

- Essential for computing screened interaction W_0.

Building on Single-Particle Green's Function G_0

$G_0 W_0$ **Approximation:**

- Calculate screened interaction W_0 from polarizability P_0.
- Compute self-energy as $\Sigma_{xc} = iG_0 W_0$.
- Common starting approximation in practical GW calculations.

Choice of Starting Hamiltonian $\hat{h}$

Importance:

- Critical to GW accuracy.
- Ideally, starting Hamiltonian approximates GW quasi-particle results.

Kohn–Sham Hamiltonian

Features:

- Common initial choice, particularly LDA or GGA.
- Provides good densities but underestimates band gaps (50-100%).
- Wavefunctions often good approximation (overlaps typically $>$95%).

Hartree–Fock Hamiltonian

Features:

- Physically meaningful eigenvalues (Koopmans' theorem).
- Significant bandgap overestimation.
- Suitable mainly for large-gap semiconductors and atoms.

Generalized Kohn–Sham Hamiltonian (8/10)

Features:

- Includes non-local exchange potentials (hybrid functionals).
- Balances ground-state properties and improved band structures.
- Popular choice for accurate GW calculations.

DFT+U Method

Features:

- Empirical approach adding gap magnitude U.
- Practical for strongly correlated materials (transition-metal oxides, lanthanides).
- Offers convenient starting point for complex correlated systems.

Summary of Hamiltonian Choices

Guidelines for selection:

- Choice strongly depends on materials and computational resources.
- Trade-off between computational efficiency and physical accuracy.
- Kohn–Sham (LDA/GGA): pragmatic but underestimates gaps.
- Hartree–Fock: accurate energies, excessive gaps.
- Generalized Kohn–Sham (hybrid functionals): balanced accuracy.
- DFT+U: practical and semi-empirical for strongly correlated systems.

Which W_0?

- GW screening often computed within RPA (Ch. 11).
- Replacing P_{RPA} by $P = P_0$ (vertex corrections) leaves formalism unchanged.
- Improvement depends on error cancellation between missing vertex corrections in P and in Σ_{xc}.

Justification for DFT-RPA W_0

- RPA screening with Kohn–Sham inputs yields ϵ^{-1} close to experiment.
- Partial error cancellation and accurate KS density underlie this success.
- Strong argument: use DFT-RPA as starting W_0.
- Beyond-RPA improvements via TDDFT or BSE (Chs. 14.11, 15.3).

Discrete-Pole Representation of W_0

A major challenge: frequency integration in $G_0 W_0$. If

$$W_0(\omega) \approx \sum_s \left(\frac{W_s^p}{\omega - \omega_s^p} + \frac{W_s^p}{\omega + \omega_s^p} \right),$$

then self-energy becomes a double sum over poles of G_0 and poles of W_0 .

Plasmon Pole Model: Motivation

- Kramers–Kronig links real/imag parts of ϵ^{-1}.
- Suffices to approximate imaginary part.
- Homogeneous electron gas: single-plasmon branch $\omega_p(q) \approx v_F q/\sqrt{3} + q^2/4$.
- Crystals: one dominant plasmon peak in loss function $-\mathrm{Im}\,\epsilon^{-1}_{GG}(q;\omega)$ at small q.

Single-Plasmon Pole: Imaginary Part

$$\operatorname{Im}\epsilon^{-1}_{GG'}(q;\omega) = -A_{GG'}(q)\left[\delta(\omega - \omega^{p}_{GG'}(q)) + \delta(\omega + \omega^{p}_{GG'}(q))\right]. \tag{11}$$

- $\omega^{p}_{GG'}(q)$: effective plasmon frequency.
- $A_{GG'}(q)$: plasmon strength.

Single-Plasmon Pole: Real Part

By Kramers–Kronig:

$$\mathrm{Re}\,\epsilon^{-1}_{GG'}(q;\omega) = \delta_{GG'} + \frac{2}{\pi}\frac{A_{GG'}(q)\,\omega^{p}_{GG'}(q)}{\omega^2 - [\omega^{p}_{GG'}(q)]^2}. \tag{12}$$

Fitting Parameters: Static Limit

Parameters A and ω^p can be determined by:

- Static limit $\omega = 0$ and f-sum rule.

Offers simple analytic determination but may introduce rigid shifts.

Fitting Parameters: Imaginary-Axis Method

Alternative: fit $\epsilon^{-1}(i\omega)$ along imaginary axis at frequencies 0 and $i\tilde{\omega}$ (order of plasmon energy).

- Yields better agreement with full-frequency RPA.
- Allows robustness checks by varying fit frequency.

Restricting Calculations to Quasi-Particle Properties

- In many GW calculations, the primary interest lies in determining quasi-particle (QP) properties, such as band structures and lifetime broadenings.
- For such purposes, the full self-energy $\Sigma(\omega)$, which is generally non-hermitian and complex, is simplified to a real, energy-dependent approximation.
- The resulting equation has the structure of a one-body Schrödinger equation for each quasi-particle state ℓ

Quasiparticle Equations

$$\left(\hat{h} + \mathrm{Re}\,\hat{\Sigma}(\varepsilon_\ell)\right)|\psi_\ell(\varepsilon_\ell)\rangle = \varepsilon_\ell|\psi_\ell(\varepsilon_\ell)\rangle. \tag{13}$$

This quasi-particle equation, when solved near the Fermi level, provides sufficient information for most practical GW band structure calculations.

Solving the Quasi-Particle Equation to First Order

- For an appropriate initial Green's function G_0, solving the quasi-particle equation to first order in the difference between the GW self-energy Σ_{xc} and the exchange-correlation potential v_{xc} is justified.
- The first-order corrected quasi-particle energies ε_ℓ are given by:

$$\varepsilon_\ell = \varepsilon_\ell^0 + \langle \psi_\ell^0 | \hat{\Sigma}_{xc}(\varepsilon_\ell) - \hat{v}_{xc} | \psi_\ell^0 \rangle, \tag{14}$$

- $|\psi_\ell^0\rangle$ are eigenstates of the independent-particle Hamiltonian $\hat{h}$.

Linearizing the Self-Energy

- To simplify the evaluation, the self-energy $\Sigma_{xc}(\omega)$ can be linearly expanded around the initial energies ε_ℓ^0.
- This yields the linearized quasi-particle equation:

$$\varepsilon_\ell = \varepsilon_\ell^0 + Z_\ell \langle \psi_\ell^0 | \hat{\Sigma}_{xc}(\varepsilon_\ell^0) - \hat{v}_{xc} | \psi_\ell^0 \rangle, \tag{15}$$

Linearizing the Self-Energy

- The renormalization factor Z_ℓ is defined by:

$$Z_\ell^{-1} = 1 - \langle \psi_\ell^0 | \frac{\partial \hat{\Sigma}_{xc}}{\partial \omega} \bigg|_{\varepsilon_\ell^0} | \psi_\ell^0 \rangle. \tag{16}$$

- The factor Z_ℓ, representing the weight of the quasi-particle in the spectral function, effectively reduces the magnitude of the self-energy correction, stabilizing and simplifying the computational treatment of the quasi-particle states.

Different Levels of Self-Consistency in GW Calculations

- The standard GW approximation (GWA), specifically the $G_0 W_0$ approach, relies on an initial Green's function G_0 derived from a static mean-field approximation.
- $G_0 W_0$ is inherently dependent on the starting point and can exhibit significant limitations, such as:
  - Dependence on initial Hamiltonian choice
  - Violation of particle number conservation
  - Poor satellite description
  - Unphysical spectral functions due to improper gap representation
- To mitigate these issues, various degrees of self-consistency have been introduced.

Alignment of the Chemical Potential

- The simplest self-consistency step is aligning the chemical potentials between the initial Green's function G_0 and the resulting GW calculation by introducing an energy shift $\Delta\varepsilon$:

$$\mu = \mu_0 + \Delta\varepsilon = \mu_0 + \Sigma_{k_F}(\mu). \tag{17}$$

- The adjusted Green's function becomes:

$$G_0^\sigma(r_1, r_2; z) = \sum_n \frac{\psi_{n\sigma}(r_1)\psi_{n\sigma}^*(r_2)}{z - \varepsilon_{n\sigma}^0 - \Delta\varepsilon}, \tag{18}$$

- with the corresponding frequency shift in the self-energy:

$$\Sigma(z) \to \Sigma(z - \Delta\varepsilon). \tag{19}$$

Z = 1 Approximation

- By assuming each state undergoes a uniform shift $\Delta\varepsilon$, one can simplify the self-consistency condition by evaluating the self-energy without the renormalization factor Z:

$$\varepsilon_\ell = \varepsilon_\ell^0 + \langle\psi_\ell^0|\hat{\Sigma}(\varepsilon_\ell^0) - \hat{v}_{xc}|\psi_\ell^0\rangle. \tag{20}$$

- This approximation avoids the detailed calculation of quasi-particle renormalization factors.

Self-Consistent Update of Quasi-Particle Energies

- A more comprehensive approach involves updating quasi-particle energies iteratively, which adjusts screening effects and typically increases the calculated gap closer to Hartree–Fock results.
- Such updates are crucial for accurate spectral predictions, especially if significant reordering of states occurs.

Self-Consistent COHSEX

- For systems where Kohn–Sham wavefunctions differ significantly from quasi-particle wavefunctions, self-consistency can be introduced using the static COHSEX approximation.
- COHSEX employs a static self-energy constructed only from occupied states, simplifying the computational effort compared to fully dynamical self-consistency.

Quasi-Particle Self-Consistent GW (QSGW)

- The QSGW method constructs an optimized static, non-local Hamiltonian H^{QP}, closely matching the GW-derived quasi-particle eigenvalues and wavefunctions. The effective Hamiltonian is defined as:

$$H^{QP} = \frac{1}{2} \sum_{ij} |\psi_i^{QP}\rangle \left[\mathrm{Re}\Sigma_{ij}(\varepsilon_i^{QP}) + \mathrm{Re}\Sigma_{ij}(\varepsilon_j^{QP}) \right] \langle \psi_j^{QP}|. \tag{21}$$

- QSGW generally provides improved predictions for quasi-particle energies and wavefunctions compared to $G_0 W_0$.

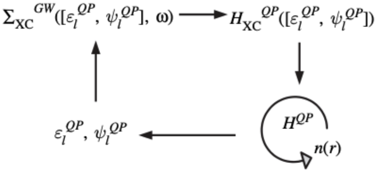

Figure 12.2. Self-consistency loop of the QSGW approach [291, 292]. From a starting dynamical GWA exchange–correlation self-energy an optimized static non-local potential is constructed. This is added to the starting Hartree hamiltonian to yield the full optimized H^{QP}. It is updated with an internal self-consistency loop on the density, which is recalculated with the eigenfunctions of H^{QP}. Finally the new quasi-particle wavefunctions and energies are used as input to update the GWA self-energy. The outer loop is cycled till convergence.

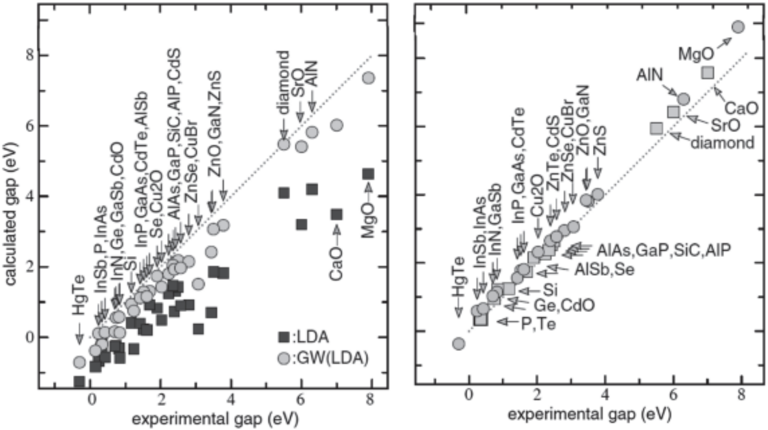

Figure 13.5. Fundamental gaps of *sp* compounds in LDA (squares) and in G_0W_0 starting from LDA (circles) in the left panel and QSGW in the right panel. All results are taken from [291]. The effects of spin–orbit coupling were subtracted from the experimental values. The G_0W_0 gaps improve on the LDA, but are still systematically underestimated and can even remain negative for small-gap semiconductors. For QSGW data, zinc-blende compounds with direct $\Gamma-\Gamma$ transitions are shown as circles; all other gaps are shown as squares. Errors are small and systematic, and would be even smaller if the electron–phonon renormalization were included; see Sec. 13.6. G_0W_0 and QSGW are defined in Sec. 12.4.

GW0 Approach

The GW0 approach performs full self-consistency in G while keeping W_0 fixed. This method conserves particle number and maintains better satellite spectra accuracy compared to fully self-consistent GW. However, it leads to results closer to Hartree–Fock due to reduced screening.

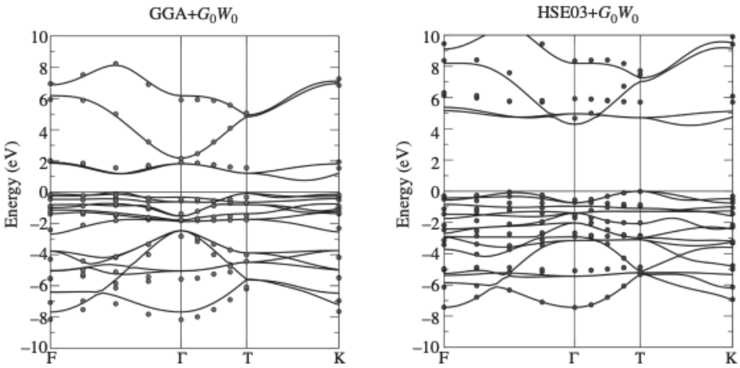

Figure 13.12. Band structure of NiO, adapted from the results of [581] by Claudia Rödl. Left panel: the continuous lines are the result of a GGA calculation. Dots denote the QP energies obtained within G_0W_0 starting from the GGA. Right panel: the continuous lines are the result of a HSE03 hybrid functional calculation. Dots as before. The valence band maximum is set to zero in both calculations. Note the starting-point dependence of the G_0W_0 results. The labels of the high-symmetry points refer to the rhombohedric cell. In the f.c.c. cell this corresponds to L (rhombohedric F), L' (rhombohedric T), and X (rhombohedric K), respectively.

Fully Self-Consistent GW

- Fully self-consistent GW calculations iteratively solve the Dyson equation for both G and W.
- While this method is essential for accurate total energy calculations, it may degrade spectral quality due to inadequate treatment of vertex corrections.
- **Rules of Thumb**:
  - The choice of self-consistency depends on the targeted properties.
  - GW0 with "best W" is often recommended for accurate spectra, combining realistic screening and correct analytical properties.
  - For total energies, fully self-consistent GW within RPA may offer preferable results.

Frequency Integrations in GW Calculations

Frequency integrations represent one of the most challenging aspects of GW calculations due to the presence of poles near the real axis. Here I present some of the different approaches:

Calculation of P_0

- The irreducible polarizability P_0 can be calculated via frequency Fourier transforms as:

$$P_0(\omega) = -\frac{i}{2\pi} \lim_{\eta \to 0^+} \sum_\sigma \int d\omega' \, G_\sigma(\omega + \omega') G_\sigma(\omega') e^{i\eta\omega'}, \tag{22}$$

- For finite temperatures using Matsubara frequencies:

$$P_0(z_n) = \frac{1}{\beta} \sum_m \sum_\sigma G_\sigma(z_m) G_\sigma(z_n + z_m). \tag{23}$$

- These equations simplify to known forms when using independent-particle Green's functions.

Plasmon Pole Approximation

A simplified integration for the self-energy Σ involves approximating the screened Coulomb interaction W using plasmon poles, particularly useful for evaluating real parts of the self-energy near the Fermi level. This approach significantly reduces computational complexity.

Full Frequency Integration (I)

Direct numerical integration of the full frequency-dependent self-energy $\Sigma(\omega)$ on the real axis is computationally demanding due to closely spaced poles. Alternatives to full real-axis integrations include:

- **Matsubara Frequencies**: At non-zero temperatures, self-energy calculations are typically performed using discrete Matsubara frequencies:

$$\Sigma(z_n) = -\frac{1}{\beta}\sum_m G(z_n - \nu_m)W(\nu_m). \tag{24}$$

- **Spectral Function Method**: At zero temperature, exploiting the analytic structure of Green's functions leads to integration via spectral functions $A(\omega)$ and $D(\omega)$:

$$\Sigma_c(\omega) = \int_{-\infty}^{+\infty} d\omega_1 \int_0^{\infty} d\omega_2 \frac{A(\omega_1)D(\omega_2)}{\omega + (\omega_2 - i\eta)\mathrm{sgn}(\mu - \omega_1) - \omega_1}. \tag{25}$$

Full Frequency Integration (II)

Other Alternatives to full real-axis integrations include:

- **Contour Integration**: Utilizing contour integration in the complex plane simplifies the evaluation significantly:

$$\Sigma_c(\omega) = -\frac{i}{2\pi}\int_{-i\infty}^{+i\infty} G(\omega+z)W_p(z)dz + \sum_i f_i(r)f_i^*(r')W_p(r',r,|\varepsilon_i-\omega|-i\eta)[\theta(\mu-\varepsilon_i)\theta(\varepsilon_i \tag{26}$$

  This method is more reliable as it avoids double-frequency integration.

- **Analytic Continuation**: Transitioning from imaginary-axis results to real-axis quantities can be done through analytic continuation, often employing Padé approximants:

$$R(z) = \frac{\sum_{i=0}^{n} a_i z^i}{\sum_{j=0}^{m} b_j z^j}, \tag{27}$$

  with appropriately chosen parameters to achieve desired precision near energy gaps.

GW Total Energy Calculations

- Total energy calculations within GW methods involve an additional frequency integration, typically via the Galitskii–Migdal formula:

$$E = \frac{1}{2\beta} \sum_{\ell\sigma} \sum_{\nu} (\varepsilon^{0}_{\ell\sigma} + z_\nu) G_{\ell\ell\sigma}(z_\nu), \quad \text{for } T \neq 0, \tag{28}$$

$$E = \frac{1}{2} \sum_{\ell\sigma} \int_{-\infty}^{\mu} d\omega (\varepsilon^{0}_{\ell\sigma} + \omega) A_{\ell\ell\sigma}(\omega), \quad \text{for } T = 0. \tag{29}$$

- Alternative evaluations using functional approaches, involving Matsubara frequencies and logarithmic functionals, are also common, especially in comparison to simpler DFT-RPA calculations.

GW Calculations in a Basis

- GW calculations involve both frequency and spatial integrations.
- While frequency integrations are unique to many-body perturbation theory, spatial integrations share commonalities with standard mean-field methods.
- This section focuses specifically on spatial integrations, emphasizing basis-set approaches to solving GW equations.

Matrix Elements (I)

- GW equations are often solved using matrix formulations.
- Given a set of normalized basis functions $\chi_m(r)$, independent-particle or quasi-particle wavefunctions can be expanded as:

$$\psi_{i\sigma}(r) = \sum_m b_{i\sigma}^m \chi_m(r). \tag{30}$$

- The two-point matrix elements in a general basis are defined as:

$$F_{n_1 n_2} = \int dr_1 dr_2 \chi_{n_1}^*(r_1) F(r_1, r_2) \chi_{n_2}(r_2). \tag{31}$$

Matrix Elements (II)

- Matrix elements in terms of independent-particle wavefunctions are given by:

$$F_{ij} = \int dr_1 dr_2 \psi_i^*(r_1) F(r_1, r_2) \psi_j(r_2). \tag{32}$$

- Four-point functions transform according to:

$$F_{n_1 n_2 n_3 n_4} = \int dr_1 dr_2 dr_3 dr_4 \chi_{n_1}^*(r_1) \chi_{n_2}^*(r_2) F(r_1, r_2, r_3, r_4) \chi_{n_3}(r_3) \chi_{n_4}(r_4). \tag{33}$$

- For the screened interaction W, we define matrix elements as:

$$W_{ki\ell j} = \int dr_1 dr_3 \psi_k^*(r_1) \psi_j(r_1) W(r_1, r_3) \psi_\ell(r_3) \psi_i^*(r_3). \tag{34}$$

- The self-energy matrix elements become:

$$\Sigma_{xc,k\ell} = i \sum_{ij} G_{ij} W_{k\ell}^{ij}. \tag{35}$$

Choice of the Basis: Plane Waves

Plane-wave bases are preferred for periodic systems due to computational convenience and diagonalization of the bare Coulomb interaction. Key integrals, such as the polarizability, are efficiently computed using Fast Fourier Transforms:

$$\tilde{\rho}_{ijk\sigma}(q+G) = \frac{1}{\sqrt{\Omega}} \int dr\, \psi^*_{ik\sigma}(r) \psi_{jk+q\sigma}(r) e^{-i(q+G)r}. \tag{36}$$

Choice of the Basis: Localized Orbitals

Localized-orbital bases (e.g., LCAO, LMTO, Gaussian orbitals) provide convenience in describing core and semi-core electrons. These bases have proven successful historically for various materials, especially those involving d and f electrons, as well as finite systems. Examples include the Linear Muffin-Tin Orbital (LMTO) and Numeric Atom-Centered Orbital (NAO) bases.

Optimized Basis for Polarizability

To reduce computational demands, the polarizability P_0 can be computed using an optimized product basis derived from pairs of orbitals. This significantly reduces the computational overhead by minimizing the number of required basis functions.

Basis for Self-Consistent Calculations

- In self-consistent GW calculations, new quasi-particle wavefunctions are most conveniently expressed in the basis of eigenfunctions derived from the initial independent-particle Hamiltonian.
- Typically, only a small subset of eigenfunctions is required since the self-energy mixing is limited to a relatively small energy range and conserves crystal momentum.

Scaling and Convergence: The Coulomb Interaction

- Careful treatment of the long-range Coulomb interaction is crucial in GW calculations.
- In plane-wave calculations for finite systems, simulations typically employ a large periodically repeated unit cell (supercell) containing the studied object surrounded by empty space.
- While ground-state calculations of neutral systems without dipole moments easily handle supercells, excited-state calculations suffer from convergence difficulties due to long-range interactions arising from electron additions, removals, or dipole creation.
- To alleviate this problem and reduce computational demands, modified Coulomb interactions cut off in real space can be employed.
- In extended systems, the steep reciprocal-space Coulomb interaction $4\pi/q^2$ presents similar issues, necessitating fine q-meshes.
- An improved integration method uses two grids: a coarse grid for density and dielectric functions, and a finer grid for the Coulomb interaction.
- This enhanced integration technique improves convergence for both periodic and finite systems, effectively managing the divergence at $q = 0$.

Important Convergence Parameters

Spectroscopy calculations, including GW0 quasi-particle or spectral function computations, require careful consideration of convergence parameters that differ significantly from ground-state calculations:

- **k-points**: While convergence is less stringent than optical calculations, rigorous testing remains necessary due to pole integrations.
- **Empty States**: Convergence with empty states is typically slow, displaying an error scaling approximately as $E_{\text{cut}}^{-3/2}$. Iterative inversion methods circumvent explicit summation over bands, implicitly defining band numbers through Hamiltonian dimensions.
- **Number of Basis Functions**: Practically, separate considerations for wavefunction expansions and self-energy summations are beneficial. Smaller inverse dielectric function components can suffice when crystal local field effects (LFE) are minimal, optimizing computational efficiency.

Scaling of GW Calculations

- Typical GW calculations employ spectral representations in plane-wave bases, with key computational steps exhibiting varied scaling behaviors:
  - Calculation of $\tilde{\rho}$ using fast Fourier transforms scales as $N_{\mathrm{at}} \ln(N_{\mathrm{at}})$.
  - Polarizability matrix element calculations scale as $N_{\mathrm{at}}^4 N_k^2$, simplifying to N_{at}^2 for smaller unit cells.
  - Single self-energy matrix elements scale as $N_q N_{\mathrm{at}}^3$ or N_{at}^2 in sufficiently small cells.
- For large systems, significant scaling improvements are achievable by employing the nearsightedness principle, which assumes spatial localization of relevant quantities.
- Real-space methods, such as the space-time approach, calculate Green's functions directly, scaling as N_{at}^2, and compute polarizabilities from Green's function products, achieving linear scaling in atom numbers.